

pubs.acs.org/est Article

Elucidating Factors Contributing to Dicamba Volatilization by Characterizing Chemical Speciation in Dried Dicamba-Amine Residues

Andromeda M. Sharkey and Kimberly M. Parker*



Cite This: *Environ. Sci. Technol.* 2024, 58, 12062–12072



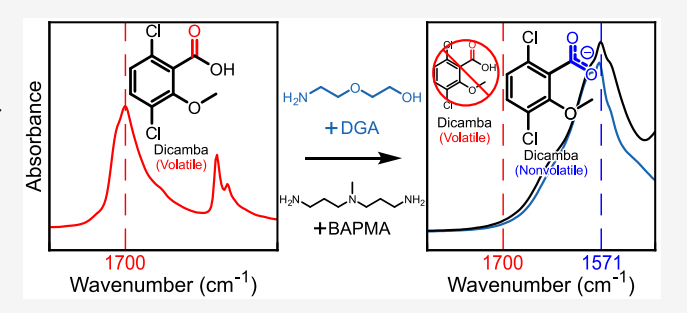
ACCESS I

III Metrics & More

Article Recommendations

Supporting Information

ABSTRACT: Dicamba is a semivolatile herbicide that has caused widespread unintentional damage to vegetation due to its volatilization from genetically engineered dicamba-tolerant crops. Strategies to reduce dicamba volatilization rely on the use of formulations containing amines, which deprotonate dicamba to generate a nonvolatile anion in aqueous solution. Dicamba volatilization in the field is also expected to occur after aqueous spray droplets dry to produce a residue; however, dicamba speciation in this phase is poorly understood. We applied Fourier transform infrared (FTIR) spectroscopy to evaluate dicamba protonation state in dried dicamba-amine residues. We first



demonstrated that commercially relevant amines such as diglycolamine (DGA) and n,n-bis(3-aminopropyl)methylamine (BAPMA) fully deprotonated dicamba when applied at an equimolar molar ratio, while dimethylamine (DMA) allowed neutral dicamba to remain detectable, which corresponded to greater dicamba volatilization. Expanding the amines tested, we determined that dicamba speciation in the residues was unrelated to solution-phase amine pK_a , but instead was affected by other amine characteristics (i.e., number of hydrogen bonding sites) that also correlated with greater dicamba volatilization. Finally, we characterized dicamba-amine residues containing an additional component (i.e., the herbicide S-metolachlor registered for use alongside dicamba) to investigate dicamba speciation in a more complex chemical environment encountered in field applications.

KEYWORDS: dicamba, volatilization, Fourier transform infrared (FTIR) spectroscopy, herbicides, amine salts

■ INTRODUCTION

Since the commercial release of glyphosate-tolerant crops in 1996, the use of herbicides on genetically modified herbicidetolerant crops has become a crucial approach to control weeds in agriculture. In recent years, the emergence of glyphosateresistant weeds has spurred the development of new genetically modified crops that tolerate herbicides with alternative modes of action to enable continued weed control.²⁻⁴ Among these, crops that tolerate the herbicide dicamba (3,6-dichloro-2-methoxybenzoic acid)⁵⁻⁷ were released in 2015, after which the use of dicamba in the U.S. increased from 3×10^6 kg in 2015 to 14×10^6 kg in 2019. Unfortunately, this increased dicamba use as a postemergent herbicide on tolerant crops has also been associated with unintentional damage to surrounding vegetation. Reports of off-target dicamba damage to nearby crops documented by the US Environmental Protection Agency (EPA) rose from none in 2016 to 3461 in 2021; the 2021 reports alone represented damage to over 1.1 million acres of cropland in 29 of the 34 states where postemergent dicamba use on dicamba-tolerant crops was approved.9 Beyond adjacent crops, the off-target movement of dicamba can damage other vegetation^{9,10} and may impact surrounding ecosystems. 11 Consequently, understanding and preventing the off-target movement of dicamba are important for both agriculture and the environment.

Off-target dicamba movement, in principle, can occur through multiple processes during or after application; ^{7,12,13} among these processes, volatilization of dicamba has been identified as an important pathway for off-target dicamba movement after application. ^{13–18} The role of volatilization has been specifically elucidated in field trials, ¹⁶ as well as emphasized in a 2021 US EPA report on dicamba off-target movement, which stated that "Officials from numerous states posit that secondary movement, or volatility, is the cause of the majority of off-target incidents." Although dicamba volatilization remains a persistent problem, efforts have been made to reduce dicamba volatilization by adding additional chemical agents to dicamba formulations. ^{7,12} These agents include

Received: February 13, 2024
Revised: April 25, 2024
Accepted: June 11, 2024
Published: June 25, 2024





amines, which deprotonate dicamba to its nonvolatile anion. ^{19,20} Amines in current dicamba formulations approved for postemergent application include diglycolamine (DGA) and n,n-bis(3-aminopropyl)methylamine (BAPMA) salts, which decrease dicamba volatilization relative to dimethylamine (DMA) and isopropylamine (IPA) formulations.²⁰ Recently, pH buffers have also been added to dicamba formulations to maintain the pH of the formulation solution above the pK_a of dicamba $(pK_a = 1.9)^{24}$ Although the inclusion of these buffers reduces dicamba volatilization compared to unbuffered solutions, 25,26 dicamba volatilization (i.e., after spray application) does not consistently correlate with solution pH, 20,26,27 suggesting that other factors beyond pH control of formulation solutions may affect volatilization. The need to consider other factors contributing to dicamba volatilization is further supported by field trials in which dicamba volatilization remained measurable from DGA and BAPMA formulations^{28,29} even when a pH buffer was added to a DGA formulation.²⁹ Additionally, there have been continued incidents of damage due to dicamba volatilization, including the 2021 reports detailed above, despite the required inclusion of DGA or BAPMA along with a pH buffer in all postemergent dicamba applications in recent years.

One possible explanation for the continued occurrence of dicamba volatilization in the field despite the use of robust strategies to control solution phase chemistry 27,30-33 is that dicamba volatilization may be occurring from a different phase-specifically, residues generated by the drying of aqueous spray droplets after application. Across typical environmental conditions, aqueous spray droplets are expected to evaporate on the order of minutes. 34-39 In contrast, dicamba volatilization occurs over several days after application, 21,29 suggesting that dicamba volatilization may continue after spray droplets have dried to a residue. Laboratory experiments have demonstrated that dicamba can volatilize from residues formed by the evaporation of aqueous solutions containing amines commonly applied with dicamba. 20,23 Comparable residues (i.e., dicamba-DGA and -BAPMA residues dried from methanol) have been identified as protic ionic liquids (PILs):⁴⁰ salts above their melting point formed by proton transfer between a Brønsted acid (e.g., dicamba) and base (e.g., amine).41 While the underlying proton transfer reaction is consistent between solutions and PILs, the extent of this reaction, as well as the factors that determine it, may differ between these phases. Specifically, for some combinations of Brønsted acids and bases, proton transfer is incomplete, resulting in the presence of both neutral and ionic species at equilibrium in the PIL. 42-46 Consistent with solution phases, neutral molecules volatize from PILs more readily than their ionic counterparts. 42,43,47 Consequently, the chemical speciation of dicamba, particularly its protonation state, in these PIL-like residues may play an important role in determining dicamba volatilization.

In this study, we investigated the protonation state of dicamba in dicamba-amine residues using Fourier Transform Infrared (FTIR) spectroscopy, which has previously been used to assess proton transfer in other condensed organic acid—base mixtures ^{48–55} including carboxylic acids (corresponding to the primary acidic moiety in dicamba) and amines. ^{52,54,55} After identifying features indicating the extent of proton transfer between dicamba and amines in residues, we tested the correlation of dicamba protonation in the residue phase with its volatilization using four amines used in commercial dicamba

formulations (i.e., DMA, IPA, DGA, and BAPMA). Using an expanded set of amines and other structurally related chemicals, we evaluated the effects of amine properties (e.g., steric factors, other functional groups) beyond amine pK_a on dicamba protonation in the residue phase. Because dicamba is often applied alongside other chemicals (e.g., other herbicides), we also used our technique to investigate the effect of an additional component (i.e., the herbicide S-metolachlor) on dicamba protonation in residues containing additional chemical constituents. Finally, we applied insights gained by our approach to identifying key factors that determine dicamba protonation in the residue phase to evaluate how they may be employed to more effectively control volatilization.

MATERIALS AND METHODS

Chemicals and Suppliers. A list of chemicals and suppliers can be found in the Supporting Information (Text S1). All herbicides and amines were used to generate concentrated stock solutions, which were subsequently employed in experiments. Concentrated amine solutions were handled in fume hoods because amines pose inhalation hazards.

Preparation of Residues for FTIR Analysis. All residues analyzed using FTIR were prepared on 25 mL PTFE evaporating dishes (Fisher Scientific, 02617146). In most experiments, residues for FTIR analysis were dried from aqueous solutions (4 mL) containing dicamba and amine at the molar ratios specified in the figure captions. In each condition, the specific amounts of dissolved chemical constituents were adjusted so that the initial masses of all constituents present summed to 5 mg. Drying was carried out over 48 h at room temperature, during which time all visible water evaporated. The final residues contained residual water, which affected residue properties, as discussed below.

Exceptions to this protocol were made in two cases. First, a small number of experiments replaced water with the solvents acetone or methanol, as discussed below. Second, residues containing S-metolachlor were dried from larger solution volumes (5–10 mL), which was required to accommodate the lower aqueous solubility of S-metolachlor (i.e., 530 mg/L, 56 or 1.9 mM, at 20 $^{\circ}\mathrm{C}$) relative to other constituents used in our study. In all cases, all visible water or solvent evaporated over the drying period.

Most dicamba residues behaved as sticky, viscous liquids (Figure S1). A smaller number instead behaved as solids, specifically: (i) dicamba free acid (FA), (ii) all dicambaethylene glycol monopropylether (EGME) residues, (iii) dicamba-DMA residues at 0.25/1 and 0.5/1 DMA/dicambamolar ratios, and (iv) dicamba-hexylamine (HA) residue at an equimolar ratio of HA to dicamba.

FTIR Analysis of Residues. FTIR spectra were collected using a Thermo Nicolet Nexus 670 spectrophotometer equipped with a Golden Gate diamond attenuated total reflection (ATR) accessory. Spectra were collected over the wavenumber range of 400–4000 cm⁻¹ at a resolution of 4 cm⁻¹. For each residue, 128 scans were averaged to generate the spectrum. When spectra were overlaid, the baseline was normalized by subtracting the absorbance at 3999 cm⁻¹ from the entire spectrum. Full FTIR spectra are presented in the Supporting Information (Figures S2–S14).

To quantitatively analyze FTIR spectra (Text S2), overlapping peaks were deconvoluted using Fityk, an open-source nonlinear peak fitting program.⁵⁷ Peaks were fit to a Voigt

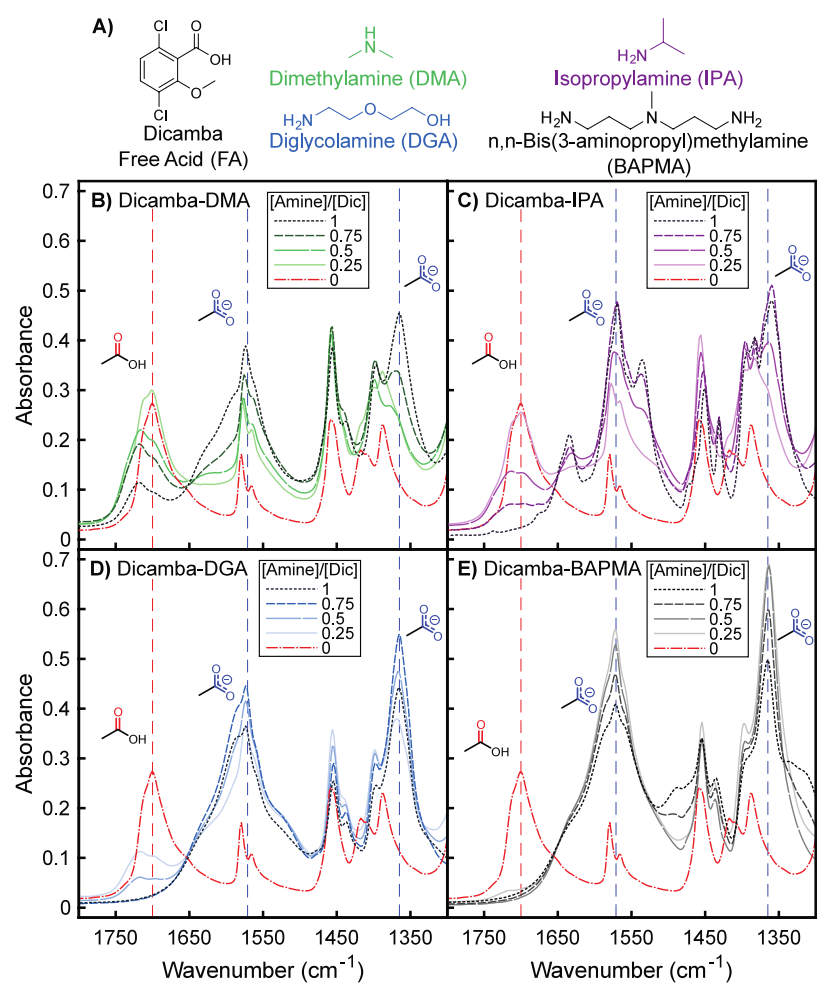


Figure 1. (A) Structures of dicamba, DMA, DGA, IPA, and BAPMA. FTIR spectra of dicamba-amine residues including (B) DMA, (C) IPA, (D) DGA, and (E) BAPMA at 0–1 amine/dicamba molar ratios ([Amine]/[Dic]). The vertical dashed red line at 1700 cm⁻¹ indicates the approximate location of the carbonyl stretching peaks, while the dashed blue lines at 1571 and 1365 cm⁻¹ indicate the approximate respective locations of asymmetric and symmetric carboxylate stretching peaks.

profile using the Levenberg–Marquardt method for solving nonlinear least-squares problems (Text S3). Deconvoluted spectra (Figures S15–S24) with corresponding probable peak assignments (Tables S1–S10) are presented in the Supporting Information, along with summary compilations presenting the peaks associated with moieties indicating dicamba protonation (i.e., carboxylic acid and carboxylate moieties) across residue compositions (Tables S11–S13, Figure S25). Because additional components (e.g., amines) dilute dicamba in addition to altering protonation, dicamba protonation was quantified as the ratio of the heights of these peaks to account for changes in the concentration of total dicamba in the final residue (Figure S26). Ratios of peak areas yielded similar results (Figure S27).

Volatilization Measurements. Dicamba volatilization measurements were performed following procedures described previously. Briefly, dicamba and amine residues for volatilization measurements were dried for 24 h at room temperature from a 2 mL solution containing 123 μ M dicamba (equivalent to 246 nmol or 54.4 μ g), the specified molar ratio of amine, and (when applicable) the specified molar ratio of Smetolachlor in a 50 mL glass beaker. After drying, two initial beakers were extracted with 2 mL of 1/1 (v/v) water/acetonitrile to determine the initial amount of dicamba, amines, or S-metolachlor present in the residue. The remaining

three beakers were placed on a hot plate at 40 °C for 48 h followed by extraction using the same protocol. Chemical concentrations in the extracts were determined using the analytical methods described below and multiplied by the volume of the extract to determine the moles of chemicals in the two initial beakers and the three final beakers. The differences in these values were used to calculate the moles of each chemical lost during the experiment.

A fraction of the extract was analyzed to determine dicamba concentrations following a published method using an Agilent 1260 high-pressure liquid chromatography instrument with UV absorbance detection (HPLC-UV) equipped with a Poroshell 120 C-18 column. For residues containing S-metolachlor, this method was adapted to quantify dicamba and S-metolachlor concentrations in the same method using a flow rate of 0.35 mL/min with 40% of 0.1% formic acid in water and 60% of 99% acetonitrile/1% water. Dicamba and S-metolachlor were eluted at 3.9 and 8.7 min, respectively, and were detected using 225 and 210 nm wavelengths, respectively. To quantify amine concentrations, a separate 300 μ L fraction of the extract was derivatized using fluorenylmethyloxycarbonyl-chloride prior to HPLC-UV analysis using previously published methods. ²³

RESULTS AND DISCUSSION

FTIR Analysis of Dicamba Free Acid (FA). Before determining how other components (i.e., amines) affect the FTIR spectra of the residues, we first identified the peaks present in an FTIR spectrum of a residue containing dicamba alone dried from water (Figure S2). This spectrum agreed well with FTIR spectra for dicamba available in databases and a prior publication. We expected that, without amines or other bases present, dicamba in this residue would be present primarily in its neutral form (i.e., dicamba free acid, FA), consistent with neutral dicamba exclusively being present in the crystal structure of dicamba FA dried from toluene determined by X-ray diffraction. 61

Examining the FTIR spectrum of dicamba FA allowed us to identify peaks that could be leveraged to differentiate neutral dicamba from the dicamba anion (i.e., peaks associated with the carboxylic acid moiety). Among assigned peaks (Figure S2), one was present at 1700 cm⁻¹, which fell within the wavenumbers associated with the carbonyls present in dimerized carboxylic acid moieties (Figure S28) attached to aromatic rings (1700–1680 cm⁻¹).⁶² A second broad peak at 916 cm⁻¹ is likely associated with the out-of-plane wag of carboxylic acid dimers (960-880 cm⁻¹).⁶² The occurrence of carboxylic acid dimers in the dicamba FA residue is in agreement with the crystal structures of dicamba FA⁶¹ and other aromatic carboxylic acids (e.g., benzoic acid). 63,64 Among peaks associated with neutral carboxylic acids, 62 we selected to use the carbonyl stretching peak at 1700 cm⁻¹ in subsequent comparisons to other residues due to the absence of other peaks in this range in the dicamba FA FTIR spectrum.

FTIR Analysis of Dicamba-Amine Residues. We next evaluated changes to the FTIR spectra upon inclusion of an amine in the residue associated with the transfer of a proton from dicamba to the amine. We included four amines (Figure 1A) used in commercial dicamba products (i.e., DMA, IPA, DGA, BAPMA)^{7,65} at increasing initial amounts up to an equimolar molar ratio to dicamba. The inclusion of all four amines reduced the size of the carbonyl peak at 1700 cm⁻¹. In addition, two new peaks appeared near 1571 and 1365 cm⁻¹; these wavenumbers fall within the ranges associated with asymmetric and symmetric stretching of carboxylate moieties, respectively 62,66 (Figure 1B-E). On the asymmetric carboxylate stretching peak near 1571 cm⁻¹, we also observed shoulders associated with protonated amine moieties; these peaks became more apparent upon deconvolution of the spectra (Figures S16-S24, Tables S1-S10). The inclusion of primary amines resulted in two shoulder peaks associated with NH₃⁺ asymmetric and symmetric bending (1625–1560 and 1550–1505 cm⁻¹, respectively),⁶⁶ while secondary amines contribute a single shoulder peak associated with NH₂⁺ bending (1620–1560 cm⁻¹).⁶⁶ Together, these changes in FTIR spectra upon the inclusion of amines in the dicamba residue are consistent with proton transfer from the carboxylic acid in dicamba to the amine.

Additional important changes in the spectra were associated with the disruption of the carboxylic acid dimer identified in dicamba FA. At higher amine/dicamba ratios, the carbonyl peak near 1700 cm⁻¹ was accompanied by a shoulder or second peak between 1730 and 1710 cm⁻¹ (Figure 1B–E). Additionally, the broad carboxylic acid dimer out-of-plane wag peak (960–875 cm⁻¹)⁶⁶ was absent in the spectra from dicamba-amine residues other than dicamba FA and both

dicamba-DMA and dicamba-IPA residues at a 0.25/1 amine/dicamba molar ratio (Figure S29). These observations agree with trends previously hypothesized to result from the preferential formation of solvated carboxylic acid monomers over dimers when certain carboxylic acids were diluted into polar solvents, ⁶³ which may occur herein when dicamba is diluted into the amine. The ability of amines to disrupt hydrogen bonding within the dicamba dimers may influence dicamba volatilization from the residue phase as well as affect the quantification of neutral dicamba in the residues (Text S3).

To evaluate the relative effects of the four amines on the protonation state in the residues, we prepared residues with lower ratios of amine relative to dicamba so that differences in the dicamba protonation state could be observed (Figure 1B-E). We first compared the effects of DMA (Figure 1B) and IPA (Figure 1C), which both contain a single amine moiety that we hypothesized would each be capable of deprotonating one dicamba molecule. The dicamba carbonyl peak remained visible in all residues prepared with excess dicamba relative to amine (Figure 1B, C), consistent with a single proton transfer from dicamba to the solitary amine moiety present in both DMA and IPA. However, the carbonyl peak was still visible when DMA was added at an equimolar ratio to dicamba (Figure 1B), but not when IPA was added at the same ratio (Figure 1C). This difference may relate to the order of the amine moieties in DMA and IPA (i.e., secondary vs primary), as detailed below.

Although DGA, like DMA and IPA, contains a solitary amine moiety, a visible carbonyl peak was absent even in some residues prepared with excess dicamba (i.e., 0.75/1 DGA/dicamba; Figure 1D). To explain the complete deprotonation of dicamba despite the stoichiometrically insufficient number of amine moieties to accept the protons, we hypothesized that another constituent (e.g., another DGA moiety, residual water in the dried residue) may be acting as a proton acceptor in these residues. Though limited to other systems, some literature supports the possibility that residual water in the residues may accept excess protons from dicamba. In one PIL, trace water was found to accept a proton from the acid to form the hydronium ion, 67 and water was also protonated when mixed at an equimolar ratio with a strong acid to generate another PIL. 68

To test the effect of residual water on dicamba protonation in residues, we prepared dried dicamba-DGA residues from methanol and acetone instead of aqueous solutions. We confirmed that dicamba-DGA residues dried from methanol and acetone had smaller water OH stretching peaks (3700-3400 cm⁻¹)⁶⁶ than those dried from water (Figure S30A), indicating that residual water in the residue largely remained from water used as the solvent rather than taken up as atmospheric water vapor due to residues acting as hydroscopic PILs.⁶⁹ We also confirmed that DGA deprotonates dicamba in residues prepared from all solvent systems by observing that the size of the carbonyl peak decreased relative to the carboxylate peaks in residues prepared with higher amounts of DGA relative to dicamba, regardless of the solvent (Figure S30B). When comparing residues prepared at the same DGA/ dicamba molar ratio in different solvents, the carbonyl peaks were substantially higher in residues dried from methanol or acetone than in residues dried from water, suggesting that residual water may contribute to additional dicamba deprotonation. In particular, at the 0.75/1 DGA/dicamba molar ratio, the carbonyl peak was observed in the dicamba-

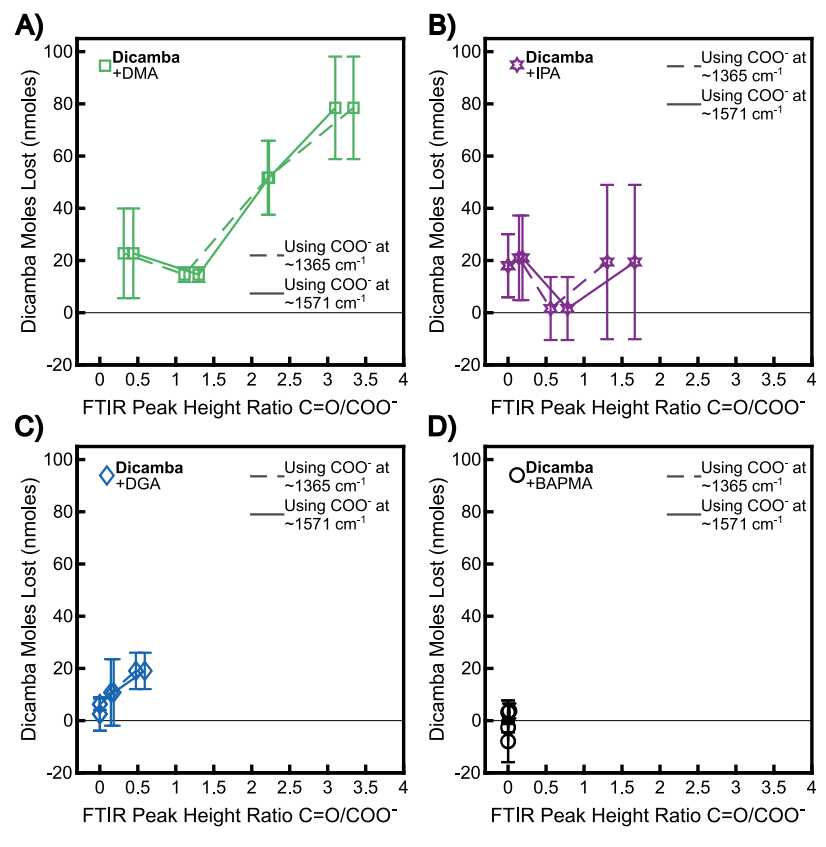


Figure 2. Comparison of dicamba lost to volatilization to the ratio of the FTIR peak heights of the carbonyl (C=O) and carboxylate (COO⁻) peaks for dicamba-amine residues prepared with (A) DMA, (B) IPA, (C) DGA, and (D) BAPMA. Measurements of dicamba volatilization and FTIR spectra were obtained from two sets of residues prepared at the same amine/dicamba ratios; these values and their corresponding peak height ratios are plotted in Figure S26. Dicamba moles lost to volatilization were calculated as the difference between the initial amount of dicamba (nominal value = 246 nmol) measured in the residue after 24 h of drying at room temperature to the final amount of dicamba present in the residue after 48 h at 40 °C. Error bars represent the propagated error of the range of the two initial dicamba measurements and the standard deviation of the three final dicamba measurements.

DGA residues dried from methanol and acetone, but not water, supporting our hypothesis that residual water, if present, may contribute to deprotonation of dicamba.

Among the amines tested, BAPMA uniquely contained multiple amine moieties (two primary amines and one tertiary amine), which we hypothesized would lead to extensive dicamba deprotonation even at low BAPMA/dicamba molar ratios. Previously, proton transfer between one BAPMA molecule and up to three dicamba molecules was observed using nuclear magnetic resonance (NMR) in dicamba-BAPMA PILs dried from methanol.⁴⁰ Consistent with our hypothesis, no carbonyl peak was observed in residues at or above a 0.5/1 BAPMA/dicamba molar ratio, while a small peak was visible in the residue prepared at a 0.25/1 BAPMA/dicamba molar ratio, which corresponded to a small excess of dicamba carboxylic acid groups relative to BAPMA amine moieties (Figure 1E). Consequently, the deprotonation of dicamba in residues containing BAPMA was consistent with the three amine moieties in BAPMA acting as proton acceptors.

Relationship of Protonation Measured by FTIR to Volatilization from Residues. To test our hypothesis that dicamba protonation correlates to its volatilization from the residues, we quantitatively compared the size of peaks associated with the carboxylic acid and carboxylate moieties on dicamba FA and dicamba anion, respectively, by calculating a ratio of peak heights to account for dilution of dicamba by the addition of the amines. As discussed in the prior section,

the height of the carbonyl peak at 1700 cm⁻¹ decreased sharply when the fraction of amine was increased due to disruption of the carboxylic acid dimer in addition to deprotonation and dilution; this change was accompanied by formation of a shoulder or second peak between 1730 and 1710 cm⁻¹ associated with the carboxylic acid monomer that was quantified alongside the dimer (Table S11, Figure S31). Because the dimer and monomer represent two distinct states in which dicamba is present in its neutral form, the heights of these peaks in the deconvoluted spectra were summed as a conservative estimate of the extent of dicamba protonation. In contrast, the carboxylate moiety in dicamba is present in a single ionic state but results in two peaks corresponding to the asymmetric stretch near 1571 cm⁻¹ and the symmetric stretch near 1365 cm⁻¹ that are highly correlated across the different residues (Table S11). Both peaks associated with the carboxylate moiety were used individually to calculate the corresponding ratios that are presented in all figures; ratios from each peak resulted in consistent trends and are not distinguished further in the following discussion. In cases where the carboxylate peaks were absent after deconvolution, the ratio was not calculated.

Loss of dicamba due to volatilization from residues over 48 h at 40 °C was measured at varying initial amine/dicamba molar ratios corresponding to those used in FTIR measurements (i.e., 0.25/1, 0.5/1, 0.75/1, 1/1) (Figure S32). The resultant trends, as well as the observed variations among replicates, were

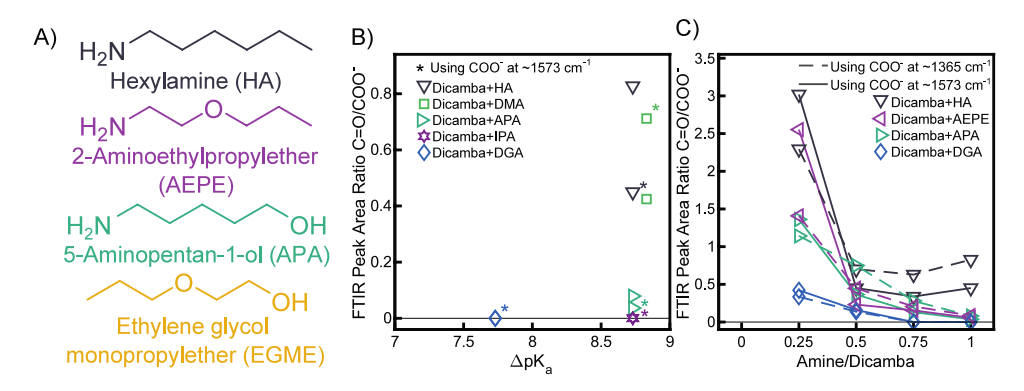


Figure 3. (A) Structures of the DGA analogues used in this study. (B) Ratio of the FTIR peak heights of the carbonyl (C=O) and carboxylate (COO⁻) peaks at approximately 1571 cm⁻¹ (labeled with asterisk) or 1365 cm⁻¹ (unlabeled) for dicamba-amine residues containing DMA, DGA, HA, and APA compared against the Δ p K_a values for the different dicamba-amine pairs. (C) Ratio of the FTIR peak heights of the carbonyl (C=O) and carboxylate (COO⁻) for dicamba-amine residues initially containing DGA, HA, APA, and AEPE at 0.25–1 molar ratios to dicamba dried from aqueous solutions on PTFE dishes.

comparable to those obtained for residues prepared with three of these amines (i.e., DMA, DGA, and BAPMA) at slightly different molar ratios (i.e., 0.1/1, 0.3/1, 0.6/1, 1/1) in a prior study.²⁰ Specifically, dicamba volatilization from residues prepared with DMA increased at lower DMA/dicamba ratios. Similar trends were seen for residues prepared with DGA, although dicamba volatilization was lower than that from DMA residues, while no dicamba volatilization was measured from residues containing BAPMA at a 0.25/1 molar ratio or higher. Dicamba volatilization from residues containing IPA at varying molar ratios had not previously been reported; contrary to our expectations, we did not find evidence that dicamba volatilization correlated with the IPA/dicamba ratios. These updated dicamba volatilization data were used in subsequent comparisons to the dicamba protonation state in residues prepared at the corresponding amine/dicamba molar ratio analyzed by FTIR.

Consistent with our hypothesis, dicamba protonation appears to serve an important but not exclusive role in determining dicamba volatilization (Figure 2). Volatilization of dicamba from residues prepared with both DMA (Figure 2A) and DGA (Figure 2C) increased as dicamba protonation shifted toward the neutral form (indicated by a higher ratio of carbonyl peak height to carboxylate peak heights). Relative to the DGA residue, more neutral dicamba was detected in the DMA residue, which corresponded to greater dicamba volatilization. In contrast, dicamba in the BAPMA-containing residue primarily occurred in its anionic form, corresponding to minimal dicamba volatilization (Figure 2D).

While dicamba volatilization from the DMA-, DGA-, and BAPMA-containing residues was consistent with dicamba protonation in the residue phase playing a major role, dicamba volatilization from the IPA-containing residue did not increase in residues containing a higher proportion of neutral dicamba (Figure 2B). In addition, dicamba volatilization was measured from some residues in which no neutral dicamba was detected (i.e., a ratio of peak heights equal to 0). One factor that might, in principle, contribute to dicamba volatilization in the absence of measured neutral dicamba is the higher temperature (i.e., 40 °C) used for volatilization experiments relative to the room temperature (i.e., ~20 °C) condition used for FTIR measurements. However, although the amount of neutral species in PILs has been reported to increase at higher temperatures, ^{47,70} the magnitude of this effect is expected to be very small over

the relevant temperature range (i.e., < 1% change in protonation state, Text S4). Another possibility is that anionic dicamba volatilized as an ionic pair or aggregate with other molecules (i.e., IPA), as has been observed to occur for other PILs. 71,72 Because more IPA was lost than dicamba during volatilization (Figure S32), this possibility cannot be excluded. Along with possible interactions between neutral molecules (e.g., hydrogen bonding within dicamba dimers that may influence volatilization from dicamba FA residues), these factors may contribute to cases in which dicamba volatilization cannot be solely attributed to its protonation state in the residue phase.

Relationship between Amine Properties and Dicamba Protonation in Residues. After confirming that dicamba protonation correlated with volatilization in most residues, we next aimed to investigate how amines influence dicamba protonation in the residue phase. In solution, dicamba protonation is expected to relate to the strength of the amine base (i.e., lower p K_h , corresponding to higher p K_a of the conjugate acid). While proton transfer in PILs can also correlate with the solution-phase pKa values of the acidic and basic constituents, 47 prior work has demonstrated that dicamba volatilization from residues did not correlate with amine pK_{a}^{20} suggesting that other factors may also affect dicamba protonation in the residue phase. This deviation is exemplified by DGA, which contains a solitary amine moiety that has a relatively low pK_a value (9.6) among amines included in our study (Table S14), yet is able to completely deprotonate dicamba even when dicamba was in excess of DGA (Figure 1D). Therefore, in addition to testing the effects of amine properties like pKa on dicamba protonation, we selected additional amines, as well as one non-amine compound, to characterize the effects of specific moieties in DGA beyond the amine (i.e., ether, hydroxyl) on dicamba protonation (Figure 3A) as detailed below.

Using this expanded set of compounds, we first evaluated the effect of amine pK_a (Table S14) on dicamba protonation in residues prepared with 1/1 molar ratios of amine/dicamba. The extent of proton transfer in PILs has previously been correlated with the difference in the pK_a values of the acid and base (ΔpK_a), with $\Delta pK_a > 10$ considered to suggest near-complete proton transfer. In all combinations of dicamba and amines included in our study, ΔpK_a values were <10, suggesting that complete proton transfer may not be assumed.

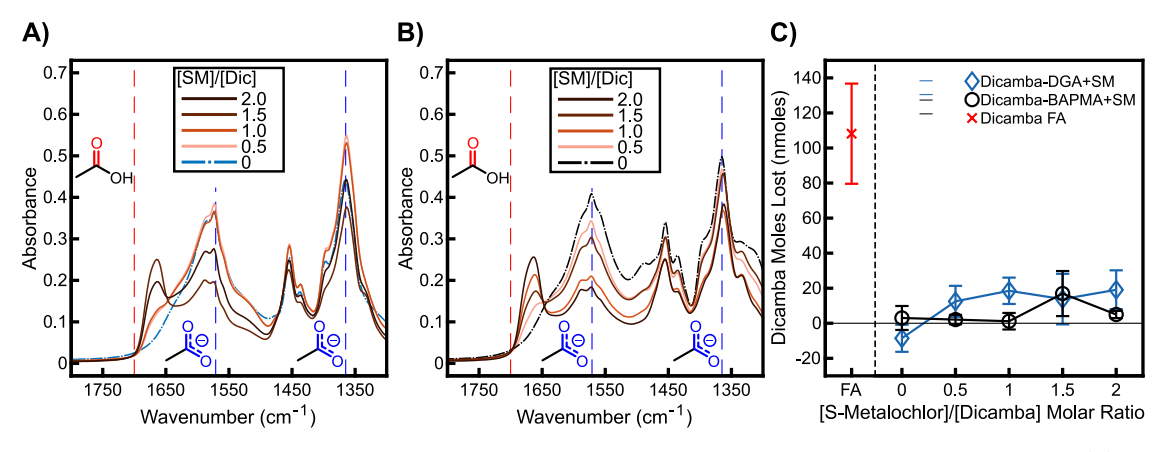


Figure 4. Spectra of dicamba-amine residues containing S-metolachlor at 0–2 S-metolachlor/dicamba molar ratios including (A) DGA and (B) BAPMA (all at 1 amine/dicamba molar ratios) dried from aqueous solutions on PTFE. The vertical dashed red line at 1700 cm⁻¹ indicates the approximate location of the carbonyl stretching peaks, while the dashed blue lines at 1571 and 1365 cm⁻¹ indicate the approximate respective locations of asymmetric and symmetric carboxylate stretching peaks. (C) Dicamba moles lost over 48 h at 40 °C from the dicamba FA and dicamba-amine residues containing S-metolachlor at 0–2 S-metolachlor/dicamba molar ratios, including DGA and BAPMA dried from water on glass. The nominal initial amount of dicamba was 246 nmoles. Error bars represent the propagated error of the range of the two initial dicamba measurements and the standard deviation of the three final dicamba measurements.

We found that $\Delta p K_a$ did not predict dicamba protonation in the residue phases (Figure 3B). Most residues prepared in our study had similar $\Delta p K_a$ values spanning a narrow range (8.7–8.8); however, the amount of dicamba in its neutral form (indicated by higher peak height ratios) varied widely among these residues. Dicamba-DGA had a lower $\Delta p K_a$ value (7.7), which is expected to correlate with less proton transfer but still did not contain measurable amounts of neutral dicamba. These results are consistent with our earlier finding that solution-phase amine $p K_a$ did not predict dicamba volatilization, ²⁰ suggesting that other factors contribute to determining dicamba protonation in and volatilization from the residue phase.

Among other contributing factors, we hypothesized that factors like amine order and other substituent effects that influence electron density and steric interactions may have increased importance in PILs due to tighter packing of molecules relative to the solution phase. Previous research on PILs found that, when combined with acetic acid, primary amines had greater extents of proton transfer compared to tertiary amines with similar pK_a values, 44,55 which was attributed to the ability of primary amines to form more stabilized bonding networks than tertiary amines. 44 A similar effect may explain the greater extent of proton transfer observed in residues prepared with IPA (a primary amine) than with DMA (a secondary amine), despite their comparable ΔpK_a values (Figure 3B). These bonding networks may be significant for other amines (e.g., BAPMA) as well. Beyond amine order, other structural features may sterically affect the ability of amines to deprotonate dicamba in the residue. For example, the long alkyl chain on hexylamine (HA) may disrupt the interactions required for proton transfer, reducing its ability to deprotonate dicamba relative to IPA (Figure 3B) despite both being primary amines with similar $\Delta p K_a$ values. This effect may contribute to the decreased ability for amines with long alkyl chains to prevent dicamba volatilization from residues.20

In addition to steric effects, we hypothesized that another factor that may affect dicamba protonation is the presence of additional polar functional groups (i.e., the ether and hydroxyl moieties in DGA). In other PILs, the inclusion of hydroxyl

groups on amine molecules increased proton transfer between the amine and an acid. 52,54 In agreement with our hypothesis, we observed that HA, which is a stronger base than DGA but lacks the ether and hydroxyl moieties (Figure 3A), is much less able to deprotonate dicamba than DGA across all amine/ dicamba molar ratios (Figure 3C). To evaluate the individual contributions of the hydroxyl group and the ether group in DGA on dicamba protonation, we obtained FTIR spectra of residues prepared with two additional DGA analogues, 5aminopentan-1-ol (APA) and 2-aminoethylpropylether (AEPE, also called 2-propoxyethylamine), that each contains only the hydroxyl or the ether moiety, respectively (Figure \$33). When added at equimolar ratios to dicamba, both APA and AEPE reduced the height of the peak associated with neutral dicamba to almost nondetectable levels, resulting in peak height ratios similar to those obtained with DGA (Figure 3C). However, at lower amine/dicamba molar ratios, the peak height ratios obtained with APA and AEPE were either similar to those obtained with HA or fell between those obtained with HA and DGA (Figure 3C). The similar results for residues prepared with APA and AEPE, which fall within the bounds for residues prepared with HA and DGA, suggest that both the hydroxyl and ether moieties contributed to DGA's ability to deprotonate dicamba.

Further experiments using ethylene glycol monopropylether (EGME), which contains the ether and hydroxyl groups but not the amine, confirmed that these groups were enhancing the ability of the amine to deprotonate dicamba but do not appear to deprotonate dicamba themselves. The addition of EGME to the residues did not affect the size of peaks, including those associated with carboxylic acid protonation, in the 1800-1300 cm⁻¹ range (Figure S33) nor the 1000-800 cm⁻¹ range (Figure S34). Because carboxylate peaks were not generated, the peak ratio was undefined and could not be plotted. Further analysis suggested that though EGME was added to the residues, it did not remain present, likely due to volatilization during the drying process. Specifically, peaks associated with EGME's ether and hydroxyl moieties (CH2-O-CH2: 1150-1085 cm⁻¹, CH₂-OH: 1075-1000 cm⁻¹)⁶² were not observable in the residue (Figure S35). In contrast, peaks attributed to ether and hydroxyl moieties were observed in

residues prepared with AEPE and APA at 1119 and 1057 cm⁻¹, respectively, while residues prepared with DGA contained both peaks (Figure S35). Consequently, the hydroxyl and ether groups appear to enhance the ability of the amine in DGA to deprotonate dicamba but do not deprotonate dicamba themselves. A possible explanation is that these polar groups, if maintained in the residue by dicamba-amine interactions, increase the retention of residual water in the residue phases, which may contribute to additional deprotonation as discussed above (Figure S30). This effect may contribute to the reported ability of polar moieties in amine molecules to contribute to reduced dicamba volatilization from the residue phase.²⁰

Dicamba Protonation in and Volatilization from Residues Containing S-Metolachlor. In addition to dicamba and amines, in practice, dicamba spray solutions frequently contain other components, including other herbicides.⁷ These additional components are also expected to become incorporated into the residue upon drying, where they may alter the protonation and volatilization of dicamba. Among possible additional components that might occur in dicamba-amine residues, we selected to investigate the impact of the herbicide S-metolachlor on dicamba protonation and volatilization in residues due to its known application alongside dicamba. Specifically, one dicamba-DGA product includes Smetolachlor at a ~1.6 S-metolachlor to dicamba molar ratio,⁷³ while two other low-volatilization dicamba products are approved to be mixed with various S-metolachlor products prior to application. Recause S-metolachlor is nonionizable,76 we hypothesized that the inclusion of Smetolachlor would have little impact on both dicamba protonation and volatilization in the residues.

To test this hypothesis, we generated dicamba-DGA and dicamba-BAPMA residues from solutions containing S-metolachlor at molar ratios to dicamba spanning 0.5/1–2/1 (Figure 4A, B), which encompasses ratios used in practice. ⁷³ In all residues, the amine/dicamba molar ratios were maintained at 1/1. The addition of S-metolachlor to dicamba-amine residues decreased the height of the dicamba carboxylate peaks; however, the peak associated with the carbonyl in neutral dicamba was not visible. Consequently, the decreasing size of the carboxylate peaks was likely due to the dilution of dicamba by the addition of S-metolachlor rather than a change in its protonation state. A new peak was observed near 1665 cm⁻¹ that is present in the spectrum of pure S-metolachlor; ⁷⁷ this peak is likely associated with the carbonyl group (1740–1650 cm⁻¹)⁶² present on the S-metolachlor structure.

Consistent with no change in dicamba protonation, S-metolachlor had little impact on dicamba volatilization (Figure 4C). The addition of S-metolachlor also did not change the amounts of DGA and BAPMA that volatilized (Figure S36). Surprisingly, we found that S-metolachlor, which was completely recovered in the initial residues after drying, was almost completely absent from residues after the volatilization period of our experiments (Figure S36); subsequent analysis indicated that this loss was most likely attributable to the volatilization of S-metolachlor itself (Text S5). S-metolachlor has a comparable pure phase vapor pressure (1.7 \times 10⁻⁶ kPa)⁵⁶ to dicamba (4.5 \times 10⁻⁶ kPa)⁷⁸ but is nonionizable,⁷⁶ which may facilitate its greater volatilization from the residues.

Environmental Implications. In this study, we demonstrated that FTIR can be used to assess the dicamba protonation state in dried residue phases, which is a key factor determining dicamba volatilization.⁷ Increasing amounts

of neutral dicamba relative to the anion correlated with increasing dicamba volatilization from residues prepared with some amines (i.e., DMA, DGA, and BAPMA). However, this correlation was not seen with other amines (i.e., IPA), suggesting that other secondary factors must be considered to explain the volatilization of dicamba from some residues. For example, intermolecular interactions involving neutral dicamba (which likely determine dicamba volatilization from dicamba FA residues) may prevent dicamba volatilization in the neutral form. In addition, deprotonated dicamba, in principle, may volatilize as an ion pair or aggregate with amines. 71,72 Consequently, our method to measure dicamba protonation in residues is applicable not only to evaluate the ability of amines to suppress dicamba volatilization via deprotonation but also to identify the cases in which dicamba volatilization from residues cannot be explained by protonation alone. This insight into chemical interactions in the residue phases may benefit the future development of formulations to suppress dicamba volatilization in the field. Our approach might also be applied to investigate residue chemistry throughout the volatilization process (e.g., changing composition due to volatilization of dicamba and/or amines²³).

Notably, the solution-phase pK_a of the amine does not predict the dicamba protonation state in the residue, consistent with prior observations that this parameter does not predict dicamba volatilization.²⁰ Additional properties of the amine that may impact dicamba protonation in residues include the number of amine groups (i.e., multiple amine groups on BAPMA), amine order (i.e., the primary amine IPA vs the secondary amine DMA), steric factors (i.e., the alkyl chain on HA), and the ability to form complex bonding networks. In particular, dicamba is deprotonated to a greater extent by amines containing additional polar groups (e.g., the hydroxyl and ether moieties on DGA), which may explain the contribution of these groups to suppressing dicamba volatilization.²⁰ Alone, as in EGME, these moieties do not affect the dicamba protonation state directly, suggesting that they instead allow the amine to more effectively deprotonate dicamba. A possible explanation for this effect is that these moieties increase the amount of water remaining in the dried residue. Dicamba-DGA residues dried from water had higher extents of proton transfer compared to residues dried from solvents (e.g., acetone), consistent with lower extents of volatilization. ²⁰ Trace water has been shown to affect the properties of other PILs (e.g., viscosity, conductivity, diffusivity, and hydrogen bonding). Onsequently, the hygroscopicity of residue constituents may play an important role in controlling dicamba protonation and volatilization. In addition, other factors (e.g., humidity, temperature) likely alter water content in the dried residue, which may contribute to the observed effects of these factors on dicamba volatilization. 16,18,84

Beyond dicamba, amine, and residual water, authentic residues generated in practice may contain other chemical constituents, including additional compounds commonly added to dicamba-containing spray solution (i.e., other herbicides, surfactants, adjuvants, volatilization, and drift-reducing agents),⁷ some of which have been observed to influence dicamba volatilization. ^{25,26,32,85} The impact of these additional constituents on dicamba protonation in residues may be employed to characterize their influence on dicamba volatilization. We demonstrated that one of these constituents, the herbicide S-metolachlor, did not affect dicamba proto-

nation in the residues, which was consistent with its negligible effect on dicamba volatilization. This approach may be applied to assess dicamba protonation in residues containing other constituents; however, peaks associated with dicamba species must be able to be differentiated from peaks contributed by other constituents for accurate analysis. Consequently, constituents like the herbicide glyphosate and acetate buffers, each of which contain carboxylic acid moieties, may require alternative techniques (e.g., NMR, computational modeling)^{40,51} to assess their impact on dicamba protonation and ultimately volatilization of dicamba in the field.^{20,26,31}

ASSOCIATED CONTENT

Supporting Information

The Supporting Information is available free of charge at https://pubs.acs.org/doi/10.1021/acs.est.4c01591.

Chemicals, suppliers, and glassware cleaning; photographs of residues; complete FTIR spectra; quantitative analysis of protonation state; spectra deconvolution protocol; deconvoluted spectra and peak assignments; dimer structure; spectra between 1000 and 800 cm $^{-1}$; analysis of residues dried from organic solvents and water; volatilization of dicamba and amines; supplementary spectra for dicamba-amine residues; effect of temperature on proton transfer extent; p K_a values for dicamba and amines; and analysis of residues containing S-metolachlor (PDF)

AUTHOR INFORMATION

Corresponding Author

Kimberly M. Parker – Department of Energy, Environmental, and Chemical Engineering, Washington University in St. Louis, St. Louis, Missouri 63130, United States;

orcid.org/0000-0002-5380-8893; Phone: (314) 935-3461; Email: kmparker@wustl.edu

Author

Andromeda M. Sharkey — Department of Energy, Environmental, and Chemical Engineering, Washington University in St. Louis, St. Louis, Missouri 63130, United States; orcid.org/0000-0002-5414-8268

Complete contact information is available at: https://pubs.acs.org/10.1021/acs.est.4c01591

Notes

The authors declare no competing financial interest.

■ ACKNOWLEDGMENTS

This work is supported by NSF CAREER Award 2046602 and the Herman Frasch Foundation. We thank Dr. Alian Wang, Quincy H. K. Qu, and Chengzheng Yong for assistance using FTIR and Anna M. Hartig for assistance with plotting figures.

REFERENCES

- (1) Baek, Y.; Bobadilla, L. K.; Giacomini, D. A.; Montgomery, J. S.; Murphy, B. P.; Tranel, P. J. Evolution of Glyphosate-Resistant Weeds. In *Reviews of Environmental Contamination and Toxicology,* Knaak, J. B., Ed.; Springer International Publishing: Cham, 2021; Vol. 255, pp. 93–128.
- (2) Waltz, E. Glyphosate Resistance Threatens Roundup Hegemony. *Nat. Biotechnol.* **2010**, 28 (6), 537–538.
- (3) Wright, T. R.; Shan, G.; Walsh, T. A.; Lira, J. M.; Cui, C.; Song, P.; Zhuang, M.; Arnold, N. L.; Lin, G.; Yau, K.; Russell, S. M.;

- Cicchillo, R. M.; Peterson, M. A.; Simpson, D. M.; Zhou, N.; Ponsamuel, J.; Zhang, Z. Robust Crop Resistance to Broadleaf and Grass Herbicides Provided by Aryloxyalkanoate Dioxygenase Transgenes. *Proc. Natl. Acad. Sci. U.S.A.* **2010**, *107* (47), 20240–20245.
- (4) Behrens, M. R.; Mutlu, N.; Chakraborty, S.; Dumitru, R.; Jiang, W. Z.; LaVallee, B. J.; Herman, P. L.; Clemente, T. E.; Weeks, D. P. Dicamba Resistance: Enlarging and Preserving Biotechnology-Based Weed Management Strategies. *Science* **2007**, *316* (5828), 1185–1188.
- (5) US Department of Agriculture-Animal and Plant Health Inspection Service. *Determination of Nonregulated Status for Monsanto Company MON 88701 Cotton.* https://www.aphis.usda.gov/brs/aphisdocs/12 18501p det.pdf (accessed 2020-06-03).
- (6) US Department of Agriculture-Animal and Plant Health Inspection Service. *Determination of Nonregulated Status for Monsanto Company MON 87708 Soybean*. https://www.aphis.usda.gov/brs/aphisdocs/10_18801p_det.pdf (accessed 2020-06-03).
- (7) Sharkey, S. M.; Williams, B. J.; Parker, K. M. Herbicide Drift from Genetically Engineered Herbicide-Tolerant Crops. *Environ. Sci. Technol.* **2021**, 55 (23), 15559–15568.
- (8) Wieben, C. M. Estimated Annual Agricultural Pesticide Use by Major Crop or Crop Group for States of the Conterminous United States, 1992–2019, 2021.
- (9) US Environmental Protection Agency; Tindall, K.; Becker, J.; Orlowski, J.; Hawkins, C.; Kells, B. Status of Over-the-Top Dicamba: Summary of 2021 Usage, Incidents and Consequences of Off-Target Movement, and Impacts of Stakeholder-Suggested Mitigations. https://www.regulations.gov/document/EPA-HQ-OPP-2020-0492-0021 (accessed 2022-07-13).
- (10) Charles, D. A Drifting Weedkiller Puts Prized Trees at Risk; NPR, 2018 (accessed 2024-02-13).
- (11) Iriart, V.; Baucom, R. S.; Ashman, T. Herbicides as Anthropogenic Drivers of Eco-evo Feedbacks in Plant Communities at the Agro-ecological Interface. *Mol. Ecol.* **2021**, *30* (21), 5406–5421.
- (12) Bish, M.; Oseland, E.; Bradley, K. Off-Target Pesticide Movement: A Review of Our Current Understanding of Drift Due to Inversions and Secondary Movement. *Weed Technol.* **2021**, *35* (3), 345–356.
- (13) Riter, L. S.; Pai, N.; Vieira, B. C.; MacInnes, A.; Reiss, R.; Hapeman, C. J.; Kruger, G. R. Conversations about the Future of Dicamba: The Science Behind Off-Target Movement. *J. Agric. Food Chem.* **2021**, *69* (48), 14435–14444.
- (14) Riter, L. S.; Sall, E. D.; Pai, N.; Beachum, C. E.; Orr, T. B. Quantifying Dicamba Volatility under Field Conditions: Part I Methodology. *J. Agric. Food Chem.* **2020**, *68* (8), 2277–2285.
- (15) Sall, E. D.; Huang, K.; Pai, N.; Schapaugh, A. W.; Honegger, J. L.; Orr, T. B.; Riter, L. S. Quantifying Dicamba Volatility under Field Conditions: Part II, Comparative Analysis of 23 Dicamba Volatility Field Trials. J. Agric. Food Chem. 2020, 68 (8), 2286–2296.
- (16) Zaccaro-Gruener, M. L.; Norsworthy, J. K.; Brabham, C. B.; Barber, L. T.; Butts, T. R.; Roberts, T. L.; Mauromoustakos, A. Evaluation of Dicamba Volatilization When Mixed with Glyphosate Using Imazethapyr as a Tracer. *Journal of Environmental Management* **2022**, 317, No. 115303.
- (17) Kruger, G. R.; Alves, G. S.; Schroeder, K.; Golus, J. A.; Reynolds, D. B.; Dodds, D. M.; Brown, A. E.; Fritz, B. K.; Hoffmann, W. C. Dicamba Off-target Movement from Applications on Soybeans at Two Growth Stages. *Agrosystems Geosciences, & Environment* **2023**, 6 (2), No. e20363.
- (18) Zaccaro-Gruener, M. L.; Norsworthy, J. K.; Brabham, C. B.; Barber, L. T.; Roberts, T. L.; Mauromoustakos, A.; Mueller, T. C. Dicamba Air Concentrations in Eastern Arkansas and Impact on Soybean. *Weed Sci.* **2023**, *71* (3), 265–277.
- (19) Behrens, R.; Lueschen, W. E. Dicamba Volatility. *Weed Sci.* **1979**, 27 (5), 486–493.
- (20) Sharkey, S. M.; Stein, A.; Parker, K. M. Hydrogen Bonding Site Number Predicts Dicamba Volatilization from Amine Salts. *Environ. Sci. Technol.* **2020**, *54* (21), 13630–13637.

- (21) Mueller, T. C.; Wright, D. R.; Remund, K. M. Effect of Formulation and Application Time of Day on Detecting Dicamba in the Air under Field Conditions. *Weed Sci.* **2013**, *61* (4), 586–593.
- (22) Egan, J. F.; Mortensen, D. A. Quantifying Vapor Drift of Dicamba Herbicides Applied to Soybean. *Environ. Toxicol. Chem.* **2012**, *31* (5), 1023–1031.
- (23) Sharkey, S. M.; Hartig, A. M.; Dang, A. J.; Chatterjee, A.; Williams, B. J.; Parker, K. M. Amine Volatilization from Herbicide Salts: Implications for Herbicide Formulations and Atmospheric Chemistry. *Environ. Sci. Technol.* **2022**, *56* (19), 13644–13653.
- (24) Abraham, W. The Other Dicamba Story: Chemistry Innovations That Reduce the Volatility Potential of an Extremely Effective Herbicide, 2018. https://www.cropscience.bayer.us/-/media/Bayer-CropScience/Country-United-States-Internet/Documents/Roundup-Ready-Xtend-Crop-System-Updates/VaporGrip_Technical_Overview_FINAL.ashx?la=en&hash=EE017561780BCBCF09789546E9ED45FF012AF4EB (accessed 2019-06-25).
- (25) Carbonari, C. A.; Costa, R. N.; Bevilaqua, N. C.; Pereira, V. G. C.; Giovanelli, B. F.; Lopez Ovejero, R. F.; Palhano, M.; Barbosa, H.; Velini, E. D. Volatilization of Standalone Dicamba and Dicamba Plus Glyphosate as Function of Volatility Reducer and Different Surfaces. *Agriculture* **2020**, *10* (11), 495.
- (26) Carbonari, C. A.; Costa, R. N.; Giovanelli, B. F.; Bevilaqua, N. C.; Palhano, M.; Barbosa, H.; Lopez Ovejero, R. F.; Velini, E. D. Volatilization of Dicamba Diglycolamine Salt in Combination with Glyphosate Formulations and Volatility Reducers in Brazil. *Agronomy* **2022**, *12* (5), 1001.
- (27) Ferreira, P. H. U.; Thiesen, L. V.; Pelegrini, G.; Ramos, M. F. T.; Pinto, M. M. D.; da Costa Ferreira, M. Physicochemical Properties, Droplet Size and Volatility of Dicamba with Herbicides and Adjuvants on Tank-Mixture. *Sci. Rep.* **2020**, *10* (1), 18833.
- (28) Jones, G. T.; Norsworthy, J. K.; Barber, T.; Gbur, E.; Kruger, G. R. Off-Target Movement of DGA and BAPMA Dicamba to Sensitive Soybean. *Weed Technol.* **2019**, 33 (1), 51–65.
- (29) Bish, M. D.; Farrell, S. T.; Lerch, R. N.; Bradley, K. W. Dicamba Losses to Air after Applications to Soybean under Stable and Nonstable Atmospheric Conditions. *J. Environ. Qual.* **2019**, 48 (6), 1675–1682.
- (30) Mueller, T. C.; Steckel, L. E. Spray Mixture pH as Affected by Dicamba, Glyphosate, and Spray Additives. *Weed Technol.* **2019**, 33 (4), 547–554.
- (31) Mueller, T. C.; Steckel, L. E. Dicamba Volatility in Humidomes as Affected by Temperature and Herbicide Treatment. *Weed Technol.* **2019**, 33 (04), 541–546.
- (32) Castner, M. C.; Norsworthy, J. K.; Roberts, T. L. Evaluation of Potassium Borate as a Volatility Reducing Agent for Dicamba. *Weed Sci.* **2022**, *70*, 610–619.
- (33) Kouame, K. B.; Butts, T. R.; Werle, R.; Johnson, W. G. Impact of Volatility Reduction Agents on Dicamba and Glyphosate Spray Solution pH, Droplet Dynamics, and Weed Control. *Pest Manag. Sci.* **2022**, *79*, 857–869.
- (34) Polli, E. G.; Alves, G. S.; de Oliveira, J. V.; Kruger, G. R. Physical—Chemical Properties, Droplet Size, and Efficacy of Dicamba Plus Glyphosate Tank Mixture Influenced by Adjuvants. *Agronomy* **2021**, *11* (7), 1321.
- (35) Oliveira, R. B.; Dario, G.; Alves, K. A.; Gandolfo, M. A. Influence of the Glyphosate Formulations on Wettability and Evaporation Time of Droplets on Different Targets. *Planta Daninha* **2015**, 33 (3), 599–606.
- (36) Xu, L.; Zhu, H.; Ozkan, H. E.; Thistle, H. W. Evaporation Rate and Development of Wetted Area of Water Droplets with and without Surfactant at Different Locations on Waxy Leaf Surfaces. *Biosystems Engineering* **2010**, *106* (1), 58–67.
- (37) de Oliveira, R. B.; Bonadio Precipito, L. M.; Gandolfo, M. A.; de Oliveira, J. V.; Lucio, F. R. Effect of Droplet Size and Leaf Surface on Retention of 2,4-D Formulations. *Crop Prot.* **2019**, *119*, 97–101.
- (38) Li, H.; Travlos, I.; Qi, L.; Kanatas, P.; Wang, P. Optimization of Herbicide Use: Study on Spreading and Evaporation Characteristics

- of Glyphosate-Organic Silicone Mixture Droplets on Weed Leaves. Agronomy 2019, 9 (9), 547.
- (39) Xu, L.; Zhu, H.; Ozkan, H. E.; Bagley, W. E.; Krause, C. R. Droplet Evaporation and Spread on Waxy and Hairy Leaves Associated with Type and Concentration of Adjuvants. *Pest Manag. Sci.* **2011**, *67* (7), 842–851.
- (40) Pernak, J.; Kaczmarek, D. K.; Rzemieniecki, T.; Niemczak, M.; Chrzanowski, Ł.; Praczyk, T. Dicamba-Based Herbicides: Herbicidal Ionic Liquids versus Commercial Forms. *J. Agric. Food Chem.* **2020**, 68 (16), 4588–4594.
- (41) Greaves, T. L.; Drummond, C. J. Protic Ionic Liquids: Evolving Structure—Property Relationships and Expanding Applications. *Chem. Rev.* **2015**, *115* (20), 11379—11448.
- (42) MacFarlane, D. R.; Pringle, J. M.; Johansson, K. M.; Forsyth, S. A.; Forsyth, M. Lewis Base Ionic Liquids. *Chem. Commun.* **2006**, *18*, 1905
- (43) Lopes, J. N. C.; Rebelo, L. P. N. Ionic Liquids and Reactive Azeotropes: The Continuity of the Aprotic and Protic Classes. *Phys. Chem. Chem. Phys.* **2010**, *12* (8), 1948.
- (44) Stoimenovski, J.; Izgorodina, E. I.; MacFarlane, D. R. Ionicity and Proton Transfer in Protic Ionic Liquids. *Phys. Chem. Chem. Phys.* **2010**, *12* (35), 10341.
- (45) Kanzaki, R.; Doi, H.; Song, X.; Hara, S.; Ishiguro, S.; Umebayashi, Y. Acid—Base Property of *N* -Methylimidazolium-Based Protic Ionic Liquids Depending on Anion. *J. Phys. Chem. B* **2012**, *116* (48), 14146—14152.
- (46) Doi, H.; Song, X.; Minofar, B.; Kanzaki, R.; Takamuku, T.; Umebayashi, Y. A New Proton Conductive Liquid with No Ions: Pseudo-Protic Ionic Liquids. *Chem.—Eur. J.* **2013**, *19* (35), 11522–11526.
- (47) Yoshizawa, M.; Xu, W.; Angell, C. A. Ionic Liquids by Proton Transfer: Vapor Pressure, Conductivity, and the Relevance of ΔpK_a from Aqueous Solutions. *J. Am. Chem. Soc.* **2003**, *125* (50), 15411–15419.
- (48) Nuthakki, B.; Greaves, T. L.; Krodkiewska, I.; Weerawardena, A.; Burgar, M. I.; Mulder, R. J.; Drummond, C. J. Protic Ionic Liquids and Ionicity. *Aust. J. Chem.* **2007**, *60* (1), 21–28.
- (49) Lv, Y.; Guo, Y.; Luo, X.; Li, H. Infrared Spectroscopic Study on Chemical and Phase Equilibrium in Triethylammonium Acetate. *Sci. China Chem.* **2012**, *55* (8), 1688–1694.
- (50) Stoimenovski, J.; Dean, P. M.; Izgorodina, E. I.; MacFarlane, D. R. Protic Pharmaceuticalionic Liquids and Solids: Aspects of Protonics. *Faraday Discuss.* **2012**, *154*, 335–352.
- (51) Cui, Y.; Yin, J.; Li, C.; Li, S.; Wang, A.; Yang, G.; Jia, Y. Experimental and Theoretical Studies on Compositions, Structures, and IR and NMR Spectra of Functionalized Protic Ionic Liquids. *Phys. Chem. Chem. Phys.* **2016**, *18* (29), 19731–19737.
- (52) Reid, J. E. S. J.; Bernardes, C. E. S.; Agapito, F.; Martins, F.; Shimizu, S.; Minas da Piedade, M. E.; Walker, A. J. Structure—Property Relationships in Protic Ionic Liquids: A Study of Solvent—Solvent and Solvent—Solute Interactions. *Phys. Chem. Chem. Phys.* **2017**, *19* (41), 28133—28138.
- (53) Shen, M.; Zhang, Y.; Chen, K.; Che, S.; Yao, J.; Li, H. Ionicity of Protic Ionic Liquid: Quantitative Measurement by Spectroscopic Methods. *J. Phys. Chem. B* **2017**, *121* (6), 1372–1376.
- (54) Mann, S. K.; Brown, S. P.; MacFarlane, D. R. Structure Effects on the Ionicity of Protic Ionic Liquids. *ChemPhysChem* **2020**, *21* (13), 1444–1454.
- (55) Aravena, R. I.; Hallett, J. P. Protic Ionic Liquids Based on Fatty Acids: A Mixture of Ionic and Non-Ionic Molecules. *J. Mol. Liq.* **2023**, 373, No. 121241.
- (56) Herbicide Handbook of the Weed Science Society of America; Beste, C. E., Ed.; 5th ed.; Weed Science Society of America: Champaign, IL, 1983.
- (57) Wojdyr, M. Fityk: A General-Purpose Peak Fitting Program. J. Appl. Crystallogr. 2010, 43 (5), 1126–1128.
- (58) SpectraBase. Dicamba SpectraBase Compound ID = ET0s8elPGqS. SpectraBase; John Wiley & Sons, Inc. https://spectrabase.

- com/compound/ET0s8elPGqS?f=#8lOhDNYQgJQ (accessed 2022-09-01).
- (59) National Institute of Advanced Industrial Science and Technology. SDBSWeb: Dicamba. https://sdbs.db.aist.go.jp/sdbs/cgi-bin/ir_disp.cgi?imgdir=ir2&fname=IR200483918TK&sdbsno=45554 (accessed 2022-11-09).
- (60) Carrizosa, M. J.; Koskinen, W. C.; del Carmen Hermosín, M. Interactions of Acidic Herbicides Bentazon and Dicamba with Organoclays. *Soil Sci. Soc. Am. J.* **2004**, *68* (6), 1863–1866.
- (61) Smith, G.; O'Reilly, E.; Kennard, C. Metal Complexes of Dicamba: The Crystal and Molecular Structures of Dicamba(3,6-Dichloro-2-Methoxybenzoic Acid) and Catena-μ-Aqua-Diaquabis(3,6-Dichloro-2-Methoxybenzoato)Zinc(II) Dihydrate. Aust. J. Chem. 1983, 36 (11), 2175.
- (62) Pretsch, E.; Bühlmann, P.; Affolter, C. Structure Determination of Organic Compounds: Tables of Spectral Data, 3rd, Revised, and Enlarged English Edition; Springer: Berlin; New York, 2000.
- (63) Davey, R. J.; Dent, G.; Mughal, R. K.; Parveen, S. Concerning the Relationship between Structural and Growth Synthons in Crystal Nucleation: Solution and Crystal Chemistry of Carboxylic Acids As Revealed through IR Spectroscopy. *Cryst. Growth Des.* **2006**, *6* (8), 1788–1796.
- (64) SpectraBase. Benzoic Acid SpectraBase Compound ID = 3KpqxKPYbC8. SpectraBase; John Wiley & Sons, Inc. https://spectrabase.com/compound/3KpqxKPYbC8 (accessed 2022-09-01).
- (65) USDA National Agricultural Statistics Service. NASS Quick Stats. https://data.nal.usda.gov/dataset/nass-quick-stats (accessed 2020-05-14).
- (66) Larkin, P. Infrared and Raman Spectroscopy: Principles and Spectral Interpretation, Second ed.; Elsevier: Amsterdam, Netherlands; Oxford, U.K.; Cambridge, MA, United States, 2018.
- (67) Yu, L.; Clifford, J.; Pham, T. T.; Almaraz, E.; Perry, F.; Caputo, G. A.; Vaden, T. D. Conductivity, Spectroscopic, and Computational Investigation of H₃O⁺ Solvation in Ionic Liquid BMIBF₄. *J. Phys. Chem. B* **2013**, *117* (23), 7057–7064.
- (68) Miran, M. S.; Yasuda, T.; Tatara, R.; Susan, M. A. B. H.; Watanabe, M. Amphoteric Water as Acid and Base for Protic Ionic Liquids and Their Electrochemical Activity When Used as Fuel Cell Electrolytes. *Faraday Discuss.* **2018**, *206*, 353–364.
- (69) Chen, Y.; Cao, Y.; Lu, X.; Zhao, C.; Yan, C.; Mu, T. Water Sorption in Protic Ionic Liquids: Correlation between Hygroscopicity and Polarity. *New J. Chem.* **2013**, *37* (7), 1959.
- (70) Chen, K.; Wang, Y.; Yao, J.; Li, H. Equilibrium in Protic Ionic Liquids: The Degree of Proton Transfer and Thermodynamic Properties. *J. Phys. Chem. B* **2018**, *122* (1), 309–315.
- (71) Zhu, X.; Wang, Y.; Li, H. Do All the Protic Ionic Liquids Exist as Molecular Aggregates in the Gas Phase? *Phys. Chem. Chem. Phys.* **2011**, *13* (39), 17445.
- (72) Horikawa, M.; Akai, N.; Kawai, A.; Shibuya, K. Vaporization of Protic Ionic Liquids Studied by Matrix-Isolation Fourier Transform Infrared Spectroscopy. *J. Phys. Chem. A* **2014**, *118* (18), 3280–3287.
- (73) US Environmental Protection Agency. Registration for A21472 Plus VaporGrip Technology EPA Reg. Number 100–1623. https://www3.epa.gov/pesticides/chem_search/ppls/000100-01623-20201027.pdf (accessed 2021-01-14).
- (74) US Environmental Protection Agency. Registration for Engenia Herbicide EPA Reg. Number 7969–472. https://www3.epa.gov/pesticides/chem_search/ppls/007969-00472-20201027.pdf (accessed 2021-01-14).
- (75) US Environmental Protection Agency. Registration for XtendiMax with VaporGrip Technology EPA Reg. Number 264–1210. https://www3.epa.gov/pesticides/chem_search/ppls/000264-01210-20201027.pdf (accessed 2021-01-14).
- (76) Gannon, T. W.; Hixson, A. C.; Weber, J. B.; Shi, W.; Yelverton, F. H.; Rufty, T. W. Sorption of Simazine and S-Metolachlor to Soils from a Chronosequence of Turfgrass Systems. *Weed Sci.* **2013**, *61* (3), 508–514.

- (77) National Institute of Advanced Industrial Science and Technology. SDBSWeb: Metolachlor. https://sdbs.db.aist.go.jp/sdbs/cgi-bin/landingpage?sdbsno=45583 (accessed 2023-02-02).
- (78) US EPA. Chemistry Dashboard. https://comptox.epa.gov/dashboard (accessed 2020-05-14).
- (79) Yaghini, N.; Nordstierna, L.; Martinelli, A. Effect of Water on the Transport Properties of Protic and Aprotic Imidazolium Ionic Liquids an Analysis of Self-Diffusivity, Conductivity, and Proton Exchange Mechanism. *Phys. Chem. Chem. Phys.* **2014**, *16* (20), 9266—9275.
- (80) Bodo, E.; Mangialardo, S.; Capitani, F.; Gontrani, L.; Leonelli, F.; Postorino, P. Interaction of a Long Alkyl Chain Protic Ionic Liquid and Water. *J. Chem. Phys.* **2014**, *140* (20), 204503.
- (81) Docampo-Álvarez, B.; Gómez-González, V.; Méndez-Morales, T.; Carrete, J.; Rodríguez, J. R.; Cabeza, Ó.; Gallego, L. J.; Varela, L. M. Mixtures of Protic Ionic Liquids and Molecular Cosolvents: A Molecular Dynamics Simulation. *J. Chem. Phys.* **2014**, *140* (21), 214502.
- (82) Yaghini, N.; Pitawala, J.; Matic, A.; Martinelli, A. Effect of Water on the Local Structure and Phase Behavior of Imidazolium-Based Protic Ionic Liquids. *J. Phys. Chem. B* **2015**, *119* (4), 1611–1622.
- (83) Stettner, T.; Gehrke, S.; Ray, P.; Kirchner, B.; Balducci, A. Water in Protic Ionic Liquids: Properties and Use of a New Class of Electrolytes for Energy-Storage Devices. *ChemSusChem* **2019**, *12* (16), 3827–3836.
- (84) Striegel, S.; Oliveira, M. C.; Arneson, N.; Conley, S. P.; Stoltenberg, D. E.; Werle, R. Spray Solution pH and Soybean Injury as Influenced by Synthetic Auxin Formulation and Spray Additives. *Weed Technol.* **2021**, *35* (1), 113–127.
- (85) Zaccaro-Gruener, M. L.; Norsworthy, J. K.; Piveta, L. B.; Barber, L. T.; Mauromoustakos, A.; Mueller, T. C.; Roberts, T. L. Use of Low Tunnels to Describe Effects of Herbicide, Adjuvant, and Target Surface on Dicamba Volatility. *Weed Technol.* **2023**, *37* (6), 617–627.